

High temperature electron transport properties in  
AlGa<sub>N</sub>/Ga<sub>N</sub> heterostructures

メタデータ	言語: English 出版者: 公開日: 2011-02-08 キーワード (Ja): キーワード (En): 作成者: KUZUHARA, Masaaki, TOKUDA, Hirokuni, YAMAZAKI, Jun メールアドレス: 所属:
URL	<a href="http://hdl.handle.net/10098/3006">http://hdl.handle.net/10098/3006</a>

# High temperature electron transport properties in AlGaIn/GaN heterostructures

H. Tokuda,<sup>a)</sup> J. Yamazaki, and M. Kuzuhara

*Department of Electrical and Electronics Engineering, University of Fukui, 3-9-1 Bunkyo, Fukui 910-8507, Japan*

(Received 18 June 2010; accepted 10 October 2010; published online 22 November 2010)

Hall electron mobility ( $\mu_H$ ) and sheet concentration ( $n_s$ ) in AlGaIn/GaN heterostructures have been measured from 77 to 1020 K. The effect of the deposited Al<sub>2</sub>O<sub>3</sub> layer is also investigated with varying its thickness. It is found that  $\mu_H$  decreases monotonously with the temperature ( $T$ ) and its dependence is well approximated with the function of  $\mu_H = 4.5 \times 10^3 \exp(-0.004T)$  in the temperatures over 350 K. The function is different from the commonly used one of  $\mu_H = AT^{-\alpha}$  ( $\alpha \sim 1.5$ ), which indicates that the mobility is not only governed by the polar optical phonon scattering but also the deformation potential scattering plays a role. The sheet electron concentration ( $n_s$ ) has a weak dependence on the temperature, that is, slightly decreases with temperature in 300–570 K and increases gradually up to 1020 K. The decrease is explained by considering the reduction in the polarization (probably both spontaneous and piezoelectric) charge and the increase seems to be due to the parallel conduction through the interface between GaN buffer layer and sapphire substrate. The dependence of sheet resistance ( $R_{sh}$ ) in AlGaIn/GaN is compared with that of n-GaN. In the low temperatures, AlGaIn/GaN shows a lower  $R_{sh}$  due to its high mobility, however, at the temperatures higher than 350 K,  $R_{sh}$  of AlGaIn/GaN becomes higher than that of n-GaN. This result implies that AlGaIn/GaN high-electron-mobility-transistors are inferior to GaN metal-semiconductor field-effect transistors in terms of higher source, drain, and channel resistances at high temperature operations, although further investigations on other performances such as output power and reliability are needed. The Al<sub>2</sub>O<sub>3</sub> deposited AlGaIn/GaN shows about 15% higher  $n_s$  than without Al<sub>2</sub>O<sub>3</sub> layer for the whole temperatures. On the contrary,  $\mu_H$  at 77 K shows a slight decrease with Al<sub>2</sub>O<sub>3</sub> deposition, which degree is not affected by the layer thickness. In the temperatures higher than 400 K,  $\mu_H$  is almost the same for with and without Al<sub>2</sub>O<sub>3</sub> layer. © 2010 American Institute of Physics. [doi:10.1063/1.3514079]

## I. INTRODUCTION

AlGaIn/GaN heterostructure is an attractive material for high power and high temperature operation of high-electron-mobility-transistors (HEMTs), which is enabled by high sheet electron concentration induced at AlGaIn/GaN interface and GaN's wide band gap. In order to extract high performance from HEMTs, intensive studies on the electron transport behavior have been made since 1990s. Many theoretical and experimental results are reported in order to increase electron mobility and control two dimensional electron gas (2DEG) density.<sup>1–11</sup> Throughout these works, it is found that Coulomb, interface roughness, and alloy scatterings dominate the mobility in the low temperatures (around 10 K), while polar optical phonon scattering plays a major role for the temperatures higher than 300 K.<sup>3–5,7–15</sup> The low temperature mobility reported so far increased year by year as 7500,<sup>1</sup> 10 250,<sup>4</sup> 51 700,<sup>5</sup> 53 300,<sup>8</sup> 60 000,<sup>9</sup> and 167 000.<sup>11</sup> The increase in mobility described above has been achieved by investigating the scattering mechanisms and improving the epitaxial layer quality. However, little is known for the transport properties in the high temperatures over 300 K, which should be investigated for practical device use. The result reported so far is limited to 870 K (Ref. 20) with measuring

the hall mobility and device characteristics.<sup>12–20</sup> In order to deepen the understanding of the device operation, it is indispensable to measure the transport properties in the higher temperatures.

In this paper, the results of temperature dependence of electron mobility and concentration in AlGaIn/GaN heterostructures measured up to 1020 K are discussed. The Al<sub>2</sub>O<sub>3</sub> layer is deposited by atomic layer deposition (ALD) on AlGaIn/GaN with varying its thickness. The dependence on the layer thickness is also investigated. In addition, the sheet resistance difference between AlGaIn/GaN and n-GaN is shown. In Sec. II, the experimental procedure is described. The experimental results and discussions are shown in Sec. III. Conclusion is given in Sec. IV.

## II. EXPERIMENTAL PROCEDURE

The used sample in the experiment is an epitaxial layer grown by metal organic chemical vapor deposition method on three inch sapphire substrate. After the growth of nucleation buffer layer, undoped GaN and undoped Al<sub>0.25</sub>Ga<sub>0.75</sub>N layers with thicknesses of 1  $\mu$ m and 25 nm, respectively, were successively grown. Mesa etch was done by reactive ion etching (RIE) using Cl<sub>2</sub> and BCl<sub>3</sub> for remaining the active region. Ohmic patterns were formed and metals consisting of Ti/Al/Mo/Au with a thickness of 15 nm/60 nm/35

<sup>a)</sup>Electronic mail: htokuda@u-fukui.ac.jp.

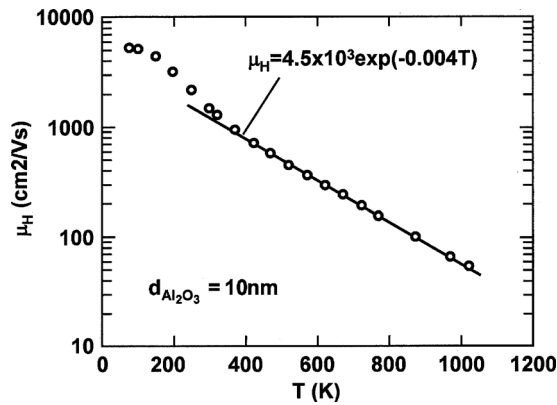


FIG. 1. Temperature dependence of hall mobility ( $\mu_H$ ) for 10 nm thick  $\text{Al}_2\text{O}_3$  deposited sample.  $\mu_H$  is well approximated with the exponential function as shown in the figure over 350 K.

nm/50 nm, respectively, were evaporated in the four corners to obtain the Van der Pauw configuration. The wafer was alloyed at 800 °C for 30 s to ensure good Ohmic contact. The processed wafer was cut into four pieces and  $\text{Al}_2\text{O}_3$  layers were deposited on three pieces of them with varying the layer thickness. The deposition was carried out by ALD system (Savannah S100-4PVP, Cambridge NanoTech) at 250 °C using trimethyl aluminum and water vapor as precursors. The thickness and refractive index were measured by ellipsometry and found to be 110 Å/1.89 (hereafter referred to as 10 nm), 318 Å/1.69 (30 nm), and 526 Å/1.67 (50 nm), respectively. After opening the window by etching  $\text{Al}_2\text{O}_3$  layer with buffered HF, the pad metals of Ti/Au (10/100 nm) were evaporated and lifted-off, completed the fabrication process. Silicon doped n-type GaN wafer was also processed with the same pattern for comparison, which did not deposit  $\text{Al}_2\text{O}_3$  layer. Its nominal carrier concentration was  $5 \times 10^{17} \text{ cm}^{-3}$  with 0.5  $\mu\text{m}$  thick. Each fabricated piece was cut to 7 × 7  $\text{mm}^2$ . The sample was set to the Hall measurement system (Toyo technica ResiTest 8310). The measurement was carried out with two steps, that is, first from 77 to 300 K and second from 300 to 1020 K. The applied magnetic field was 0.55 T. Ohmic characteristics were checked for each temperature before the measurement to ensure the reliability and reproducibility. All the measurements could be done with a current of 2 mA for 77–300 K, 0.2 mA for 300–520 K, and 0.02 mA for 570–1020 K for AlGaIn/GaN. As for n-GaN, the measurements were carried out at 2 mA for the whole temperatures. The correlation factor ( $f$ ) was larger than 0.98 for all the measurements. After the measurement at 1020 K, the sample was cooled down to the room temperature and measured again to confirm the repeatability. The room temperature sheet electron concentration and mobility were decreased by 12% and increased by 9%, respectively as compared with those in the first measurement. Similar phenomena showing the irreversible change by thermal stress are reported.<sup>16,20</sup> The values shown in the followings are the measured ones in the first for each temperature.

### III. RESULTS AND DISCUSSIONS

Figure 1 shows the temperature dependence of the hall mobility ( $\mu_H$ ) for 10 nm thick  $\text{Al}_2\text{O}_3$  deposited sample.  $\mu_H$  is

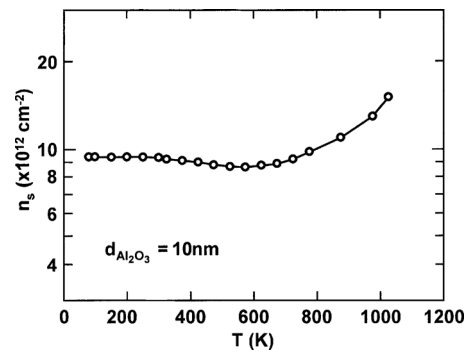


FIG. 2. Temperature dependence of sheet electron concentration ( $n_s$ ) for 10 nm thick  $\text{Al}_2\text{O}_3$  deposited sample.  $n_s$  is almost constant in 77–300 K, then slightly decreases with temperature in 300–570 K and turns to increase gradually up to 1020 K.

5200  $\text{cm}^2/\text{V s}$  at 77 K and decreases monotonously to 54  $\text{cm}^2/\text{V s}$  at 1020 K. It is well known that the mobility over 300 K is dominated by a polar optical phonon scattering<sup>12–15,20–22</sup> and it has a temperature dependence expressed as  $\mu_H = AT^{-\alpha}$ ,<sup>12,14,15,20,21</sup> where  $A$  and  $\alpha$  are the constants, or  $\mu_H = A \exp(\beta/T)$  ( $\beta$  is constant).<sup>22</sup> The reported values of  $\alpha$  scatter from 1.0 to 2.5. The fitting with these functions, however, is not sufficient and well fitted temperature regions are relatively narrow. Several attempts are made for obtaining better fitting function. It is found that the dependence is well approximated with the function of  $\mu_H = 4.5 \times 10^3 \exp(-0.004T)$  in the wide temperature range from 350 to 1020 K (see Fig. 1). In order to make the scattering mechanism clear, the proportion of the mobility in GaN is calculated by considering ionized impurity, neutral impurity, dislocation, deformation potential, piezoelectric, and polar optical phonon scatterings.<sup>23</sup> It is found that polar optical phonon scattering governs about 70%–80% and deformation potential scattering 10% at temperatures higher than 350 K. Other scatterings are negligible at high temperatures. Therefore, the mobility is not determined not only by the polar optical phonon scattering but also deformation potential scattering plays a role. The combined these two scatterings show the temperature dependence and are well fitted with the exponential function described above.

Figure 2 shows the temperature dependence of sheet electron concentration ( $n_s$ ) for 10 nm  $\text{Al}_2\text{O}_3$  deposited sample. As can be seen in the figure,  $n_s$  is almost constant of  $9.4 \times 10^{12} \text{ cm}^{-2}$  in the temperatures 77–300 K. It slightly decreases in 300–570 K and has a minimum of  $8.6 \times 10^{12} \text{ cm}^{-2}$  at 570 K. Over 570 K,  $n_s$  turns to gradual increase and shows the value of  $1.5 \times 10^{13} \text{ cm}^{-2}$  at 1020 K. A calculation is done for the temperature dependence of  $n_s$  using the simple model shown in Fig. 3.<sup>2,24</sup> The figure shows the schematic conduction band diagram and the distribution of the charges at AlGaIn/GaN heterostructure with bias voltage of 0 V, where  $\Phi_B$  is the surface barrier height,  $V_{\text{AlGaIn}}$  is the voltage across the AlGaIn layer,  $\Delta E_c$  is the band discontinuity between AlGaIn and GaN and  $\Delta E_i$  is the potential difference between the Fermi level ( $E_f$ ) and conduction band edge of GaN at the interface. Since AlGaIn layer is undoped, it is assumed that there are no donor charges in AlGaIn layer.

Equation (1) is obtained from the voltage relation

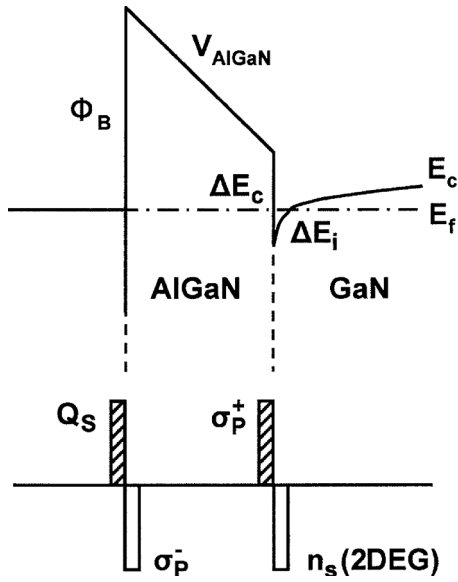


FIG. 3. Schematic conduction band diagram (upper) and distribution of the charges (lower) at AlGaIn/GaN heterostructure with bias voltage of 0 V.

$$\Phi_B - V_{\text{AlGaIn}} - \Delta E_c + \Delta E_i = 0. \quad (1)$$

The charge neutrality and electric flux continuity relations give the following Eq. (2) and (3), respectively

$$Q_s + \sigma_p^+ = \sigma_p^- + qn_s, \quad (2)$$

$$\sigma_p^+ + qn_s = \epsilon_0 \epsilon_{\text{AlGaIn}} V_{\text{AlGaIn}} / d_{\text{AlGaIn}}, \quad (3)$$

where  $Q_s$  is the surface state density ( $\text{C}/\text{cm}^2$ ),  $\sigma_p^+$  and  $\sigma_p^-$  are the polarization charge density ( $\text{C}/\text{cm}^2$ , including spontaneous and piezoelectric polarization),  $n_s$  is the sheet charge density induced at AlGaIn/GaN interface (2DEG),  $\epsilon_0$  is the permittivity of free space,  $\epsilon_{\text{AlGaIn}}$  is the dielectric constant of AlGaIn, and  $d_{\text{AlGaIn}}$  is a thickness of AlGaIn layer (25 nm in this work).

$n_s$  is calculated by the following equation:

$$n_s = N_s \exp(-\Delta E_i / kT), \quad (4)$$

where  $N_s$  is the density of state at the conduction band edge of GaN and expressed as  $N_s = m^* kT / (\pi \hbar^2)$ ,  $k$  is the Boltzmann's constant,  $T$  is the absolute temperature,  $m^*$  is an electron effective mass ( $=0.20m_0$ ) and  $\hbar$  is a Planck's constant divided by  $2\pi$ . Here, a two-dimensional density of state is assumed, although it is incorrect at high temperatures.

From Eqs. (1)–(4),  $n_s$  is calculated as a function of temperature. In the calculation,  $\Phi_B = 1.6$  eV is assumed.<sup>25</sup> Other parameters such as  $\sigma_p^+$  ( $\sigma_p^-$ ),  $\Delta E_c$ ,  $m^*$ , and  $\epsilon_{\text{AlGaIn}}$  are found in Ref. 26 and they (including  $\Phi_B$ ) are assumed to be temperature independent. Table I shows the calculated and measured  $n_s$  for several temperatures. As is shown in Table I, the calculated result explains the decrease/increase dependence, however, the difference of  $n_s$  at 77 and 570 K ( $5.5 \times 10^{10} \text{ cm}^{-2}$ ) is too small as compared with the experimental results ( $7.5 \times 10^{12} \text{ cm}^{-2}$ ). Therefore, the observed temperature dependence is not explained quantitatively with the above mentioned simple model. In order to explain larger decrease in  $n_s$ , another mechanism such as the reduction in

TABLE I. Calculated and measured sheet electron concentrations,  $n_s$  calculations and  $n_s$  measurements, respectively, for several temperatures. Although the calculated results explain the decrease/increase tendency, the difference is too small as compared with the experimental ones.

$T$ (K)	$n_s$ calc. ( $\times 10^{12} \text{ cm}^{-2}$ )	$n_s$ meas. ( $\times 10^{12} \text{ cm}^{-2}$ )
77	11.335	9.38
100	11.328	9.37
200	11.306	9.37
300	11.292	9.31
420	11.283	8.97
520	11.280	8.67
570	11.279	8.63
620	11.280	8.73
720	11.282	9.18
870	11.290	11.10
970	11.297	12.90
1020	11.301	15.10

polarization has to be taken into account. Since the lattice is expanded with the increase in temperature, the reduction in the polarization charge seems to be probable.<sup>19,27,28</sup> If assuming the reduction in  $\sigma_p^+$  and  $\sigma_p^-$  with temperature,  $n_s$  has the decreasing dependence and can be fitted with experimental results by adjusting the polarization charges at each temperature. However, the increase in  $n_s$  observed in the high temperatures is not explained by the reduction in the polarization charge. A parallel conduction through the interface between GaN buffer layer and sapphire substrate may play a role which is often observed.<sup>9,18,19,22</sup> Regarding the temperature dependence of  $n_s$ , two different tendencies have been reported, that is, monotonous increase with temperature<sup>1,4,5,9,13</sup> and decrease/increase dependence similar to Fig. 2.<sup>19</sup> The monotonous increase are observed in the relatively small Al composition ( $x < 0.20$ ) of AlGaIn/GaN structure, while decrease/increase dependence is observed in high Al composition of 0.3, which indicates that the polarization is weak from the beginning in the small Al composition structure. Therefore, it is plausible that the decrease in  $n_s$  is not observed in case of low Al composition.

The temperature dependence of sheet resistance ( $R_{\text{sh}}$ ) is shown in Fig. 4, where the result of n-GaN is also shown for comparison. The inset in the figure displays the temperature dependence of the mobility and sheet electron concentration of n-GaN.  $R_{\text{sh}}$  ( $=1/qn_s\mu_{\text{H}}$ ) of AlGaIn/GaN is smaller than that of n-GaN in the temperatures below 350 K due to AlGaIn/GaN's high mobility. However,  $R_{\text{sh}}$  of AlGaIn/GaN increases drastically in the temperatures over 500 K, while that of n-GaN has a weak dependence. As a result, almost four times higher  $R_{\text{sh}}$  is observed for AlGaIn/GaN as compared with n-GaN at 1020 K. This is because  $n_s$  in n-GaN increases monotonously with temperature and  $\mu_{\text{H}}$  decreases with rather weak dependence ( $\mu_{\text{H}} \propto T^{-1.3}$ ). The higher  $R_{\text{sh}}$  leads to the higher source, channel and drain resistances and resulting in the decrease in transconductance in the actual HEMT devices. Therefore, the result shown in Fig. 4 implies that AlGaIn/GaN HEMTs are inferior to GaN metal-semiconductor field-effect transistors (MESFETs) in terms of

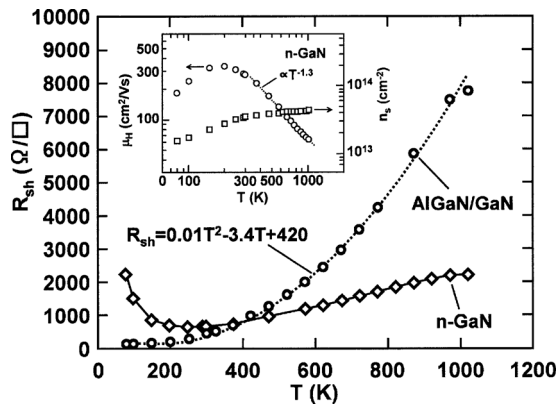


FIG. 4. Temperature dependence of sheet resistance ( $R_{sh}$ ) for AlGaIn/GaN (open circles) and n-GaN (diamonds). The inset shows that of  $\mu_H$  and  $n_s$  for n-GaN.  $R_{sh}$  in AlGaIn/GaN is well approximated with the second order polynomial for the whole temperature range.  $R_{sh}$  of AlGaIn/GaN and n-GaN crosses at 350 K.

high channel resistance at high temperature operations, although further investigations on other performances such as output power, reliability are needed. The crossing temperature of  $R_{sh}$  can be changed by varying the composition, thickness, doping concentration of AlGaIn layer, however, it seems to be difficult to obtain a lower  $R_{sh}$  with AlGaIn/GaN structures as compared with properly designed n-GaN layer in the temperatures higher than 600 K. It is to be noted that  $R_{sh}$  of AlGaIn/GaN is well approximated with a second order polynomial,  $R_{sh} = 0.01T^2 - 3.4T + 420$  for the whole temperature range (see Fig. 4). Finding this kind of analytical equation becomes a useful tool for the design of practical device.

The dependence of the deposited  $Al_2O_3$  thickness is shown in Figs. 5(a) and 5(b). The  $Al_2O_3$  deposited AlGaIn/GaN shows about 15%–30% higher  $n_s$  than without  $Al_2O_3$  layer for the whole temperatures. On the contrary,  $\mu_H$  at 77 K shows a slight decrease with  $Al_2O_3$  deposition, which degree is not affected by the layer thickness. In the temperatures higher than 400 K,  $\mu_H$  is almost the same for with and without  $Al_2O_3$  layer. The tendencies described above do not depend on the layer thickness, but dominated by with and without  $Al_2O_3$  layer. Several results are reported on the change in  $\mu_H$  and  $n_s$  with the deposition of insulating layer.<sup>19,27,29–34</sup> The results show that the device performance is improved by the deposition of insulating layer brought from the increase in  $n_s$ , which leads to the reduction in source and drain resistances. Three hypotheses are presented as the mechanism of  $n_s$  increase; (i)  $\Phi_B$  decrease with the deposition,<sup>32–34,36</sup> (ii) surface state density reduction,<sup>19,29,35</sup> and (iii) increase in polarized charge.<sup>27,28,35</sup> It is difficult to determine, whichever the correct origin is, from the obtained results in this work. This is because the increase in  $n_s$  can be explained by assuming proper values of  $\Phi_B$ , surface state or polarized charge density.

#### IV. CONCLUSIONS

Hall electron mobility ( $\mu_H$ ) and sheet concentration ( $n_s$ ) in AlGaIn/GaN heterostructures have been measured from 77 to 1020 K. The effect of the deposited  $Al_2O_3$  layer is also investigated with varying its thickness. It is found that  $\mu_H$

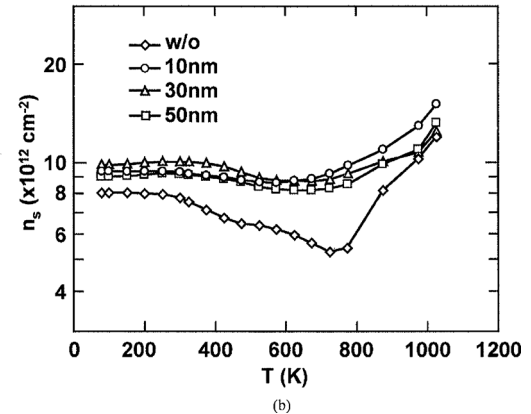
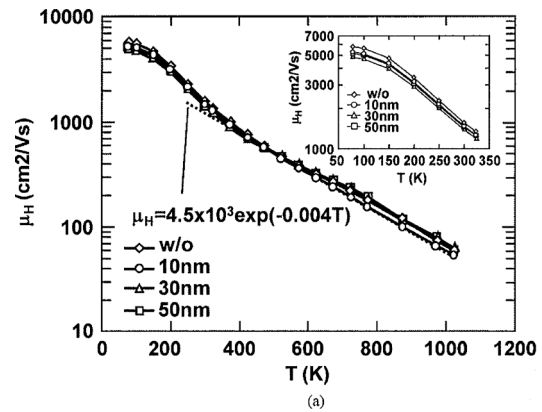


FIG. 5. Temperature dependence of  $\mu_H$  (a) and  $n_s$  (b) for different  $Al_2O_3$  thickness. Open circles, triangles and squares correspond to thickness of 10 nm, 30 nm, and 50 nm, respectively. The diamonds are the results for without  $Al_2O_3$  layer. The inset in (a) shows the dependence in a magnified scale in the temperatures 77–325 K.

decreases monotonously with the temperature ( $T$ ) and its dependence is well approximated with the function of  $\mu_H = 4.5 \times 10^3 \exp(-0.004T)$  in the temperatures over 350 K. The result indicates that the mobility is not only governed by the polar optical phonon scattering but also the deformation potential scattering plays a role. The sheet electron concentration ( $n_s$ ) has a weak dependence on the temperature, that is, almost constant in 77–300 K, then slightly decreases with temperature in 300–570 K and turns to increase gradually up to 1020 K. The decrease is explained by considering the reduction in the polarization (probably both spontaneous and piezoelectric), however, the reason of the increase is not clear. The parallel conduction at the interface between GaN buffer layer and substrate may be the origin. The dependence of sheet resistance ( $R_{sh}$ ) is well approximated with the second order polynomial for the whole temperature range. The dependence of  $R_{sh}$  in AlGaIn/GaN is compared with that of n-GaN. In the low temperatures, AlGaIn/GaN shows a lower  $R_{sh}$  due to its high mobility, however, at the temperatures higher than 350 K,  $R_{sh}$  of AlGaIn/GaN becomes higher than that of n-GaN. This result implies that AlGaIn/GaN HEMTs is inferior to GaN MESFETs in terms of source, drain, and channel resistances at high temperature operations, although further investigations on other performances such as output power and reliability are needed. The  $Al_2O_3$  deposited AlGaIn/GaN shows about 15% higher  $n_s$  than without  $Al_2O_3$  layer for the whole temperatures. On the contrary,  $\mu_H$  at 77

K shows a slight decrease with Al<sub>2</sub>O<sub>3</sub> deposition, which degree is not affected by the layer thickness. In the temperatures higher than 400 K,  $\mu_H$  is almost the same for with and without Al<sub>2</sub>O<sub>3</sub> layer. The results obtained in this work will contribute to the design of AlGaN/GaN HEMTs at high temperature operations.

- <sup>1</sup>J. M. Redwing, M. A. Tischler, J. S. Flynn, S. Elhamri, M. Ahoujja, R. S. Newrock, and W. C. Mitchel, *Appl. Phys. Lett.* **69**, 963 (1996).
- <sup>2</sup>E. T. Yu, G. J. Sullivan, P. M. Asbeck, C. D. Wang, D. Qiao, and S. S. Lau, *Appl. Phys. Lett.* **71**, 2794 (1997).
- <sup>3</sup>L. Hsu and W. Walukiewicz, *Phys. Rev. B* **56**, 1520 (1997).
- <sup>4</sup>R. Gaska, J. W. Yang, A. Osinsky, Q. Chen, M. A. Khan, A. O. Orlov, G. L. Snider, and M. S. Shur, *Appl. Phys. Lett.* **72**, 707 (1998).
- <sup>5</sup>I. P. Smorchkova, C. R. Elsass, J. P. Ibbetson, R. Vetry, B. Heying, P. Fini, E. Haus, S. P. DenBaars, J. S. Speck, and U. K. Mishra, *J. Appl. Phys.* **86**, 4520 (1999).
- <sup>6</sup>O. Ambacher, J. Smart, J. R. Shealy, N. G. Weimann, K. Chu, M. Murphy, W. J. Schaff, L. F. Eastman, R. Dimitrov, L. Wittmer, M. Stutzmann, W. Rieger, and J. Hilsenbeck, *J. Appl. Phys.* **85**, 3222 (1999).
- <sup>7</sup>Y. Zhang and J. Singh, *J. Appl. Phys.* **85**, 587 (1999).
- <sup>8</sup>M. J. Manfra, L. N. Pfeiffer, K. W. West, H. L. Stormer, K. W. Baldwin, J. W. P. Hsu, D. V. Lang, and R. J. Molnar, *Appl. Phys. Lett.* **77**, 2888 (2000).
- <sup>9</sup>E. Frayssinet, W. Knap, P. Lorenzini, N. Grandjean, J. Massies, C. Skierbiszewski, T. Suski, I. Grzegory, S. Porowski, G. Simin, X. Hu, M. A. Khan, M. S. Shur, R. Gaska, and D. Maude, *Appl. Phys. Lett.* **77**, 2551 (2000).
- <sup>10</sup>L. Hsu and W. Walukiewicz, *J. Appl. Phys.* **89**, 1783 (2001).
- <sup>11</sup>M. J. Manfra, K. W. Baldwin, A. M. Sergent, K. W. West, R. J. Molnar, and J. Caissie, *Appl. Phys. Lett.* **85**, 5394 (2004).
- <sup>12</sup>H. Lu, P. Sandvik, A. Vertiatchikh, J. Tucker, and A. Elasser, *J. Appl. Phys.* **99**, 114510 (2006).
- <sup>13</sup>N. Maeda, K. Tsubaki, T. Saitoh, and N. Kobayashi, *Appl. Phys. Lett.* **79**, 1634 (2001).
- <sup>14</sup>Z. H. Liu, S. Arulkumaran, and G. I. Ng, *Appl. Phys. Lett.* **94**, 142105 (2009).
- <sup>15</sup>A. Pérez-Tomás, M. Placidi, N. Baron, S. Chenot, Y. Cordier, J. C. Moreno, A. Constant, P. Godignon, and J. Millán, *J. Appl. Phys.* **106**, 074519 (2009).
- <sup>16</sup>S. Arulkumaran, T. Egawa, H. Ishikawa, and T. Jimbo, *Appl. Phys. Lett.* **80**, 2186 (2002).
- <sup>17</sup>M. Florovič, P. Kordoš, D. Donoval, D. Gregušová, and J. Kováč, *J. Electr. Eng.* **59**, 53 (2008).
- <sup>18</sup>M. G. Cheong, K. S. Kim, C. S. Oh, N. W. Namgung, G. M. Yang, C. H. Hong, K. Y. Kim, E. K. Suh, K. S. Nahm, H. J. Lee, D. H. Lim, and A. Yoshikawa, *Appl. Phys. Lett.* **77**, 2557 (2000).
- <sup>19</sup>D. J. Chen, Y. Q. Tao, C. Chen, R. Zhang, Y. D. Zheng, M. J. Wang, B. Shen, Z. H. Li, G. Jiao, and T. S. Chen, *Appl. Phys. Lett.* **89**, 252104 (2006).
- <sup>20</sup>I. Daumiller, C. Kirchner, M. Kamp, K. J. Ebeling, and E. Kohn, *IEEE Electron Device Lett.* **20**, 448 (1999).
- <sup>21</sup>L. Wang, W. D. Hu, X. S. Chen, and W. Lu, *J. Appl. Phys.* **108**, 054501 (2010).
- <sup>22</sup>S. B. Lisesivdin, A. Yildiz, N. Balkan, M. Kasap, S. Ozcelik, and E. Ozbay, *J. Appl. Phys.* **108**, 013712 (2010).
- <sup>23</sup>H. Tokuda, K. Kodama, and M. Kuzuhara, *Appl. Phys. Lett.* **96**, 252103 (2010).
- <sup>24</sup>J. P. Ibbetson, P. T. Fini, K. D. Ness, S. P. DenBaars, J. S. Speck, and U. K. Mishra, *Appl. Phys. Lett.* **77**, 250 (2000).
- <sup>25</sup>H. W. Jang, C. H. Jeon, K. H. Kim, J. K. Kim, S. B. Bae, J. H. Lee, J. W. Choi, and J. L. Lee, *Appl. Phys. Lett.* **81**, 1249 (2002).
- <sup>26</sup>H. Morkoç, *Handbook of Nitride Semiconductors and Devices* (Wiley-VCH, Weinheim, 2009), Vol. 3, p. 378.
- <sup>27</sup>F. G.-P. Flores, C. Rivera, and E. Muñoz, *Appl. Phys. Lett.* **95**, 203504 (2009).
- <sup>28</sup>M. Azize and T. Palacios, *J. Appl. Phys.* **108**, 023707 (2010).
- <sup>29</sup>X. Z. Dang, E. T. Yu, E. J. Piner, and B. T. McDermott, *J. Appl. Phys.* **90**, 1357 (2001).
- <sup>30</sup>S. C. Binari, K. Ikossi, J. A. Roussos, W. Kruppa, D. Park, H. B. Dietrich, D. D. Koleske, A. E. Wickenden, and R. L. Henry, *IEEE Trans. Electron Devices* **48**, 465 (2001).
- <sup>31</sup>M. Higashiwaki, N. Hirose, and T. Matsui, *IEEE Electron Device Lett.* **26**, 139 (2005).
- <sup>32</sup>N. Maeda, M. Hiroki, N. Watanabe, Y. Oda, H. Yokoyama, T. Yagi, T. Makimoto, T. Enoki, and T. Kobayashi, *Jpn. J. Appl. Phys., Part 1* **46**, 547 (2007).
- <sup>33</sup>M. Higashiwaki, N. Onojima, T. Matsui, and T. Mimura, *J. Appl. Phys.* **100**, 033714 (2006).
- <sup>34</sup>C. M. Jeon and L. L. Lee, *Appl. Phys. Lett.* **86**, 172101 (2005).
- <sup>35</sup>G. Koley and M. G. Spencer, *Appl. Phys. Lett.* **86**, 042107 (2005).
- <sup>36</sup>M. S. Miao, J. R. Weber, and C. G. Van de Walle, *J. Appl. Phys.* **107**, 123713 (2010).